Contents lists available at SciOpen

Food Science and Human Wellness

journal homepage: https://www.sciopen.com/journal/2097-0765

China Food Publishing Co.

Acer truncatum seed oil and *Rosa roxburghii* juice submicron emulsion: preparation and its therapeutic potential in alleviating scopolamine-induced memory impairment in mice

Xianting Ran[1], Liangqun Li[1], Mei Peng, Linghui Ruan, Lilang Li , Yu Wang, Jiafu Cao*, Juan Yang*

State Key Laboratory of Discovery and Utilization of Functional Components in Traditional Chinese Medicine, Natural Products Research Center of Guizhou Province, Guizhou Medical University, Guiyang 550014, China

ARTICLE INFO

Article history:
Received 14 June 2024
Received in revised form 20 July 2024
Accepted 28 August 2024

Keywords:
Acer truncatum seed oil
Rose roxburghii Tratt juice
Submicron emulsion
Scopolamine
Memory impairment

ABSTRACT

This study aimed to develop a submicron emulsion (SE) of *Acer truncatum* seed oil (ASO) and *Rose roxburghii* Tratt juice (RRTJ) using a response surface method for optimal formula screening and process parameters. The stability of ASO-RRTJ/SE and its effects on scopolamine-induced memory impairment in mice were investigated. The ASO-RRTJ/SE exhibited a desirable particle size ((276.86 ± 4.61) nm), polydispersity index (PDI, 0.22 ± 0.02), centrifugal stability parameter (*K*e, 0.143 ± 0.004), and Zeta potential ((30.57 ± 2.38) mV). Morris water maze test, measurement of acetylcholine (ACh) concentration and acetylcholinesterase (AChE) activity in the hippocampus, superoxide dismutase (SOD) activity and malondialdehyde (MDA) concentration in serum, hematoxylin and eosin (H&E) staining, immunofluorescence staining were adopt to evaluate ASO-RRTJ/SE therapeutic potential in alleviating scopolamine-induced memory impairment in mice. Behavioral tests demonstrated that ASO-RRTJ/SE significantly ameliorated scopolamine-induced spatial learning and memory deficits in mice, suggesting potential neuroprotective effects against scopolamine-mediated central nervous system excitation. Compared to the Model group, the high-dose ASO-RRTJ/SE (H-SE) group displayed a 77.84% increase in hippocampal ACh content, a 46.97% decrease in AChE activity, a 29.48% increase in serum SOD activity, and a 40.15% decrease in MDA content. H&E staining of hippocampal sections revealed that the H-SE group exhibited well-organized hippocampal neurons, with a significantly reversal of nuclear pyknosis, deep staining, and cytoplasmic dissolution. The pyramidal cell layer displayed improved organization, and the intercellular distance returned to normal. Additionally, H-SE treatment significantly reduced the aggregation of phosphorylated Tau protein, increased choline acetyltransferase expression, and promoted brain-derived neurotrophic factor production. In conclusion, ASO-RRTJ/SE ameliorates scopolamine-induced memory impairment in mice.

1. Introduction

With the accelerated pace of modern society and the explosive growth of information, the importance of memory is becoming increasingly prominent. However, due to various factors such as age, illness, or drug side effects, memory impairment issues are gradually emerging, profoundly impacting personal life and work. Consequently, research on enhancing brain function, slowing the progression of neurological diseases, and developing functional products is receiving increasing attention.

[1] X.T. Ran and L.Q. Li contributed equally to this work.

* Corresponding author at: State Key Laboratory of Discovery and Utilization of Functional Components in Traditional Chinese Medicine, Natural Products Research Center of Guizhou Province, Guizhou Medical University, Guiyang 550014, China.
E-mail address: yangxz2002@126.com (J. Yang); caojiafu1985@163.com (J.F. Cao)

Peer review under responsibility of Beijing Academy of Food Sciences.

SciOpen Publishing services by Tsinghua University Press

http://doi.org/10.26599/FSHW.2024.9250404

Acer truncatum seed oil (ASO) is a functional oil extracted from the seed kernel of *A. truncatum*, officially listed as a new resource food in China in March 2011. It is rich in unsaturated fatty acids, particularly containing 5.2%−6.2% nervonic acid[1-2], making it one of the few edible vegetable oils that contain this acid. Nervonic acid is considered the core natural component of brain nerve fibers and nerve cells[3-4], which can promote the repair and regeneration of damaged nerve tissue. Multiple studies have confirmed that ASO can reduce symptoms of depression in depressed model mice and improve the production of memory and synaptic proteins by activating certain signaling pathways[5-8], thereby contributing to the improvement of memory. The beneficial effects of ASO on human health, particularly brain health, have garnered widespread attention from the medical and technological communities.

A recent investigation has established an association with oxidative stress-driven harm and the progression of neurodegenerative diseases, further indicating that laboratory animals exhibiting superior antioxidant abilities tend to possess superior memory capabilities[9-10]. *Rose roxburghii* (RRT), abundant in Guizhou, China, boasts an impressive vitamin C content ranging from 841.5 to 3 541.1 mg/100 g in its juice, far exceeding that of kiwi and lemon, thus earning the reputation of "king of vitamin C" [11]. As a rich source of natural antioxidants, *R. roxburghii* juice (RRTJ) offers multiple health benefits, including antioxidant[12], regulation of dyslipidemia[13], and protective effect on alcoholic liver injury[14].

In terms of improving memory, the combination of ASO and RRTJ may hold unique potential. The nervonic acid component of ASO aids in the repair and development of the brain's nervous system[7,15], while the antioxidant properties of RRTJ may provide a healthier environment for the brain. However, traditional applications of ASO have been limited by its unpleasant taste, low intestinal absorption and utilization rate, and susceptibility to oxidation and deterioration[16-17].

To overcome these limitations and enhance the resource utilization value of ASO and RRT, this study employs advanced submicro emulsification technology to finely disperse ASO in RRTJ, preparing it into a submicron emulsion. This formulation not only helps improve the bioavailability of ASO but also protects it from oxidative damage through the antioxidant components of RRT. More importantly, the synergistic effect of nervonic acid and the beneficial components in RRT may jointly enhance the effect of improving memory.

This study is the first to combine ASO and RRTJ into a submicron emulsion and deeply explores its role in improving memory. This innovative research promises new breakthroughs in food applications and offers a new, natural treatment option for patients with memory impairments. Through scientific methods and rigorous experimental design, we look forward to unveiling the unique potential of this combination in improving memory.

2. Materials and methods

2.1 Reagents and materials

ASO was bought from Guizhou Xuande Biotechnology Co., Ltd. (Guiyang, Guizhou, China). RRTJ was bought from Guizhou Saisi *Rosa roxburghii* Health Industry Co., Ltd. (Duyun, Guizhou, China). Sodium starch octenyl succinateand (SSOS) was gained from Jialishi Additives (Haian) Co., Ltd. (Nantong, Jiangsu, China).

Scopolamine with 98% purity was purchased from MUST (Chengdu) Biotechnology Co. (Chengdu, Sichuan, China). Malondialdehyde (MDA), acetylcholinesterase (AChE), superoxide dismutase (SOD) and acetylcholine (ACh) assay kits were purchased from Nanjing Jiancheng Bioengineering Institute (Nanjing, Jiangsu, China). Tubulin-associated unit (Tau), choline acetyltransferase (ChAT) and brain-derived neurotrophic factor (BDNF) antibodies were purchased from Servicebio (Wuhan, Hubei, China).

2.2 Experimental animals

Male ICR mice, aged 6−8 weeks and weighing (18 ± 22) g (Speiford (Beijing) Biotechnology Co., Ltd., Beijing, China) were maintained under controlled environmental conditions at 22−26 °C with a 12 h light/dark cycle and provided with ad libitum access to food and water. All experimental procedures were carried out in strict adherence to the ethical standards outlined by the Institutional Animal Care and Use Committee (IACUC), and the protocols were duly authorized by the Animal Experiment Ethics Committee of Guizhou Medical University, under the permit number 2101015.

2.3 Formulation of ASO and RRTP submicron emulsion (ASO-RRTJ/SE)

2.3.1 Choosing of emulsifiers

A total of 17 emulsifiers listed in the National Standard for Food Safety, Standard for the Use of Food Additives (GB 2760−2014) were chosen, the emulsifier that could prepare stable oil-water mixture of ASO and RRTP without phase separation was adopted.

2.3.2 Choosing of the weight to volume ratio of ASO and RRTJ

Without the addition of emulsifier, the ten mixture of ASO and RRTJ in the proportions (g/mL) of 1:1, 1:2, 1:3, 1:4, 1:5, 1:6, 1:7, 1:8, 1:9, 1:10 were carried out by using a SCIENTZ-IID ultrasonic cell cracker (Ningbo SCIENTZ Biotechnology Co., Ltd., Ningbo, China). The optimum proportion was determined by observation of parameters, centrifugal results and centrifugal stability coefficient (*K*e).

2.3.3 Choosing of the proportion of emulsifier and co-emulsifier

Glycerol was selected as emulsifier. The mass ratio of emulsifier to co-emulsifier of 4:1, 4:3, 2:1, 1:1 was choose. The optimum proportion was determined by observation of parameters, centrifugal results and *K*e.

2.3.4 Determinaton of centrifugal stability parameter

The calculation of centrifugal stability parameter was performed according to Xie et al.[18]. ASO-RRTJ/SE was centrifuged in a HERMLE centrifuge (model Z36K, Wihingen, Germany), then, the lower layer solution was removed and mixed to a constant volume. The absorbance of the solution (*A*) was determined by UV-Vis photometer (UV-1800, shimadzu, Japan) at 500 nm. The

absorbance of the ASO-RRTJ/SE without centrifugation treated (A_0) was determined by the same method, and the centrifugal stability parameter (*K*e) was calculated as follows formula:

$$Ke = \frac{A_0 - A}{A_0} \quad (1)$$

2.4 Optimization of the preparation process for ASO-RRTJ/SE

ASO was mixed with a specified amount of SSOS and glycerin to obtain an oil solution, then the RRTJ, serving as an aqueous solution, was then added in a predetermined volume. The mixture was pre-emulsified using an ultrasonic cell disruptor at set ultrasound power and duration. The emulsion was subsequently formed employing using a 3000plus microfluidizer high pressure homogenizer (Guian New Area Ruicheng Bioengineering Co., Ltd., Guiyang, China) at set pressure. This process yielded the submicron emulsion of ASO and RRTJ.

2.4.1 Single-factor optimization of ASO-RRTJ/SE process

In order to find the best process parameters for ASO-RRTJ/SE, in our study of the submicron emulsion process, the effects of added amount of SSOS (1%, 2%, 3%, 4%, 5%), ultrasound time (1, 2, 3, 4, 5 min), ultrasonic power (200, 250, 300, 350, 400 W), and homogenization pressure (500, 1 000, 1 500, 2 000, 2 500 MPa), on the *K*e, particle size, and polydispersity index (PDI) were investigated. In each single-factor trial, one contributing factor was studied while keeping the other parameters unchanged. Each experiment was performed 3 times.

2.4.2 Response surface method (RSM) of ASO-RRTJ/SE process

According to the response surface Box–Behnken design principle, the ASO-RRTJ/SE process was optimized by taking particle size (*Y*) as the response value and selecting added amount of SSOS (*A*), ultrasound time (*B*), and homogenization pressure (*C*) as independent variables, which had a greater impact on ASO-RRTJ/SE process in a single-factor test. The design factors and levels are shown in Table 1.

Table 1
RSM design factors and levels of subcritical extraction.

Factor levels	*A*: Added amount of SSOS (%)	*B*: Ultrasound time (min)	*C*: Homogenization pressure (MPa)
−1	3	2	500
0	4	3	1 000
1	5	4	1 500

2.5 Characterization of ASO-RRTJ/SE

2.5.1 Determinaton of centrifugal retention rate

A total of 8 mL ASO-RRTJ/SE was accurately added into the graduated centrifuge tube and centrifuged for 15 min at 4 000 r/min. After centrifugation, the oil height in the upper layer was measured with a ruler. Each sample was determined three times and the data recorded. The centrifugal retention rate was calculated as follows formula:

$$\text{The centrifugal retention rate (\%)} = \frac{H - h}{h} \times 100 \quad (2)$$

Where, *H* was sample height (mL), *h* was oil height (mL)[19].

2.5.2 Determination of particle dimensions, distribution, and Zeta potential

The dimensional characteristics, including particle size and its distribution, as well as the surface Zeta potential of ASO-RRTJ/SE, were evaluated utilizing a dynamic light scattering (DLS) analyzer (NanoBrook 90Plus PALS, USA). Test samples were diluted with purified water at a ratio of 1:500. ASO-RRTJ/SE was stored at different temperatures (4, 25, 40 °C) for 15 days, and the particle size and PDI value of ASO-RRTJ/SE under these storage conditions were measured.

2.6 Animals and the experimental protocol of improving memory

After acclimatization for 1 week, the mice were randomly divided into 9 groups (10 mice per group): Control, Scopolamine (Model), Donepezil (DON, positive drug), ASO, RRTJ, ASO+RRTJ (ML), low, middle, high dose groups of ASO-RRTJ/SE (named L-SE, M-SE, H-SE, respectively). The dose selection of ASO-RRTJ/SE was based on the following considerations, Specifically, the recommended daily intake of ASO for humans is 10−20 g. After scientific dose conversion, this intake corresponds to 1.75 g/kg in the mouse model. Considering the general gavage volume for mice is 0.1 mL/10 g, we carefully designed a 5:1 emulsion ratio of RRTJ to ASO for gavage to ensure that mice could ingest a dose of ASO close to 1.75 g/kg. Based on this, we used this dose as the high-dose group and carefully prepared medium and low-dose groups by sequentially diluting the emulsion with water in half. On days 1−46, the Control and Model groups were given normal saline orally, the other groups were administered with 0.1 mL/10 g of body weight corresponding drugs by gavage continuously: DON (1 mg/kg DON), ASO (1 g ASO and 5 mL water were mixed before use), RRTJ (*R. roxburghii* juice), ML (1 g ASO and 5 mL RRTJ were mixed before use), H-SE (ASO-RRTJ/SE), M-SE (H-SE was diluted twice with water), L-SE (M-SE was diluted twice with water). The mice were weighed every 5 days. On day 32, Control group was administered with normal saline instead of the scopolamine, the other groups were intraperitoneally injected with 100 mg/kg scopolamine saline solution[20] until the end of the 46th day. On the final day, the mice were given the scopolamine again 30 min before the behavioral experiment.

2.7 Morris water maze (MWM) test

The MWM consists of a circular pool (120 cm in diameter and 40 cm in height) and image tracking software (Beijing Gene & I Technology Co., Ltd., Beijing, China). The pool is divided into 4 quadrants on average. One of the quadrants was designated as the target quadrant. A hidden platform (2 cm below the water surface)

was placed in the target quadrant. The time taken by mice to reach the platform was recorded on from the 1st to 5th days to measure escape latency. If the mouse failed to find the platform in the quadrant within 60 s, it was guided to the platform with a stick and stayed there for 30 s, and the escape latency was recorded as 60 s. On the 6th day, the hidden platform in the target quadrant was removed, and the space exploration experiment was carried out. The total distance completed in 60 s, the number of platform passes, and the residence time in the target quadrant were recorded by the software[21].

2.8 Measurement of ACh concentration and AChE activity in the hippocampus

The hippocampus of mice was excised from brain tissue, accurately weighed, and stored in a −80 °C freezer. Subsequently, the activity of AChE and the concentration of ACh in the hippocampus were quantified using the instructions provided by the reagent kit from Nanjing Jiancheng Biotechnology Research Institute (China).

2.9 Assessment of SOD activity and MDA concentration in serum

Blood samples were collected from mice through eyeball removal and subsequently centrifuged at 3 500 r/min for 10 min at 4 °C. The resulting supernatant was isolated as serum. The activity of SOD and the concentration of MDA were determined using the guidelines provided with the kit obtained from Nanjing Jiancheng Bioengineering Institute.

2.10 Hematoxylin and eosin (H&E) staining

At the end of the behavioral experiment, the mice were sacrificed, and the hippocampal tissues of the mice were removed completely and quickly on ice, and fixed with 4% paraformaldehyde at room temperature. Subsequently, paraffin-embedded, sectioned, stained, observed and photographed. The hippocampi, having undergone H&E staining, were analyzed under a light microscope (Nikon DS-U3, originating from Japan).

2.11 Immunofluorescence staining

Immunofluorescence staining analysis was conducted to quantify the expression levels of p-tau, ChAT, and BDNF in brain slices containing the hippocampus. The brain tissue samples were rinsed with normal saline, fixed in a solution containing 4% paraformaldehyde, and 4 μm thick coronal brain slices containing the hippocampus were prepared. The slices were permeabilized with 0.5% Triton X-100 in PBS for 15 min and incubated with primary antibodies at 4 °C overnight. On the following day, the coronal brain slices were rinsed with PBS at room temperature and incubated with fluorescent secondary antibody for 2 h, followed by DAPI staining for 10 min. Finally, the brain slices were observed using a fluorescence microscope and analyzed with ImageJ software. The positive rate was calculated using the formula:

$$\text{Positive rate (\%)} = \frac{\text{Positive cell count}}{\text{Total cell count}} \times 100 \quad (3)$$

2.12 Statistical analysis

The obtained results were expressed as mean ± standard deviation. Graphical representations were generated using GraphPad Prism 9 software. The statistical significance of the experimental outcomes was assessed using the least significant difference (LSD) test and the Duncan test, with a significance level set at $P < 0.05$, and these analyses were conducted in SPSS 19.0. Additionally, the experimental design and further statistical evaluations were conducted utilizing the Design-Expert software, version 13.

3. Results and discussion

3.1 Determination of ASO-RRTJ/SE formula

The difficulty of preparing ASO-RRTJ/SE is how to get the emulsifier which is soluble in ASO as well as in RRTJ. The results showed that the oil-water mixture of ASO and RRTJ which prepared with SSOS as emulsifier, was centrifuged at 4 000 r/min at room temperature for 15 min, there was absence of phase separation and with the best emulsifying effect. So SSOS was determined to be the emulsifier in ASO-RRTJ/SE formula. The addition of coemulsifier made the interface between ASO and RRTJ form a stable interface film, and reduced the interface tension sufficiently, thus the ASO-RRTJ/SE with smaller particle size and physical stability was prepared[22]. In the absence of emulsifiers, the mass ratio of ASO to RRTJ were selected by evaluating the state of oil-water mixture and Ke after centrifugation using a cell cracker. The results showed that the ratio of ASO and RRTJ were 1:5 and 1:6, no phase separation was observed, indicating a relative balance between ASO and RRTJ could be achieved without emulsifier. Considering the *K*e (0.394 and 0.689, respectively), the ratio of 1:5 was selected for the follow-up experiment. The results of the mass ratio of SSOS and glycerin showed that the ratio of SSOS and glycerin was 4:3, there was absence of phase separation and *K*e value was 0.427. However, the phase separation were observed in the other three ratios, so the mass ratio of 4:3 was adopted.

3.2 Optimization of the preparation process of ASO-RRTJ/SE

In the single-factor experiment, the amount of emulsifier, ultrasonic time, and homogenization pressure had great effects on the particle size of ASO-RRTJ/SE, therefore, the amount of emulsifier (*A*), ultrasonic time (*B*) and homogeneous pressure (*C*) were selected as the response factors, and a response surface experiment with 3 factors and 3 levels was designed using Design Expert 8.0.6 software to optimize the optimal preparation process of ASO-RRTJ/SE.

The experimental plan and results were shown in Table 2, and the results of the analysis of variance were shown in Table 3. Using Design Expert 13 software to perform regression fitting analysis on the experimental results, the regression equation was determined to be $Y = 281.5 + 3.31A - 3.78B - 3.20C + 9.17AB - 0.33AC - 6.55BC + 15.90A^2 + 10.82B^2 + 25.51C^2$. According to Table 3, the mismatch term $P = 0.181\ 0 > 0.05$ indicating that the mismatch was not significant, indicating that the established model could be used to predict the impact of preparation conditions (emulsifier dosage,

ultrasonic time and homogenization pressure) on particle size. R^2 = 0.984 6, indicated that 98.46% of the change in particle size came from the selected factors. Therefore, the order of influence of factors *A*, *B* and *C* on particle size of ASO-RRTJ/SE was *B* > *A* > *C*; that is, ultrasonic time > the amount of emulsifier > homogenization pressure, each factor had significant effect on particle size ($P < 0.05$).

Table 2

RSM design scheme and experimental results.

Number	*A* (%)	*B* (min)	*C* (MPa)	Particle size (nm)
1	−1	−1	0	316.08
2	1	−1	0	308.23
3	−1	1	0	289.85
4	1	1	0	318.70
5	−1	0	−1	322.56
6	1	0	−1	325.95
7	−1	0	1	320.52
8	1	0	1	322.60
9	0	−1	−1	319.96
10	0	1	−1	325.80
11	0	−1	1	322.94
12	0	1	1	302.60
13	0	0	0	284.77
14	0	0	0	280.85
15	0	0	0	283.77
16	0	0	0	279.52
17	0	0	0	278.60

Table 3

RSM analysis of variance results.

Source	Sum of squares	Df	Mean square	*F*-value	*P*-value	Significance
Model	5 525.59	9	612.84	49.63	< 0.000 1	***
A	87.58	1	87.58	7.09	0.032 3	*
B	114.46	1	114.46	9.27	0.018 7	*
C	81.98	1	81.98	6.64	0.036 6	*
AB	336.72	1	336.72	27.27	0.001 2	**
AC	0.43	1	0.43	0.035	0.857 4	
BC	171.35	1	171.35	13.88	0.007 4	**
A^2	1 064.16	1	1 064.16	86.18	< 0.000 1	***
B^2	492.50	1	492.5	39.89	0.000 4	***
C^2	2 739.56	1	2 739.56	221.86	< 0.000 1	***
Residual	86.44	7	12.35			
Lack of fit	57.84	3	19.28	2.70	0.181 0	
Pure error	28.60	4	7.15			
Cor total	15 602.02	16				

Note: Df, degrees of freedom. Significant effect on particle size, *$P < 0.05$, **$P < 0.01$, ***$P < 0.001$.

While keeping other factors constant, two interaction factors were selected for response surface analysis of the particle size of ASO-RRTJ/SE. A response surface graph was generated using Design Expert 8.0.6 software (Fig. 1). The results showed that the interaction between *A* and *B*, *B* and *C* were significant; that is, the effect of amount of emulsifier and ultrasonic time, ultrasonic time and homogeneous pressure on the particle size of ASO-RRTJ/SE were significant.

In order to verify the accuracy of the model prediction, the response surface optimization process was used. Combined with the convenience of practical operation, the amount of emulsifier of 4%, the ultrasonic time of 3.5 min, and the homogeneous pressure of 1 000 MPa were selected as the best preparation processes for ASO-RRTJ/SE. We carried out 3 parallel validation tests according to the process conditions. The particle size of ASO-RRTJ/SE was (276.86 ± 4.61) nm, which was close to the predicted value. Therefore, this method could be used for the preparation of ASO-RRTJ/SE.

3.3 Stability study of ASO-RRTJ/SE

Submicron emulsion is a colloidal dispersion system, which is formed by the dispersion of 1−1 000 nm droplets in another liquid, and belongs to thermodynamic instability system[23-24]. Stability is crucial for the application of submicron emulsions. The physical and chemical properties of ASO-RRTJ/SE were analyzed based on its appearance, centrifugal test and *K*e value, centrifugal retention rate, particle size and PDI, Zeta potential. Additionally, the storage stability of ASO-RRTJ/SE was also investigated.

ASO-RRTJ/SE was a light yellow, homogeneous and stable emulsion liquid with good fluidity as shown in Fig. 2A. Under the microscope, spherical emulsion droplets with complete structure and clear boundary were observed. As revealed in Figs. 2B-C, the results of methylene blue and Sudan III staining showed that ASO-RRTJ/SE was an oil-in-water (O/W) emulsion.

After centrifugation for 15 min at 4 000 r/min, there was absence of phase separation and oil droplets appearance. The *K*e value and the centrifugal retention rate are the indexes to evaluate the centrifugal stability of submicron emulsion samples. The *K*e of ASO-RRTJ/SE was 0.143 ± 0.004, the centrifugal retention rate was (90.76 ± 1.54)%. The particle size and PDI are important factors affecting the quality of submicron emulsion, and are also the key indexes to evaluate its stability and safety[25]. Low PDI values indicate uniform particle size distribution. Commonly, PDI < 0.3 is a standard value. The particle

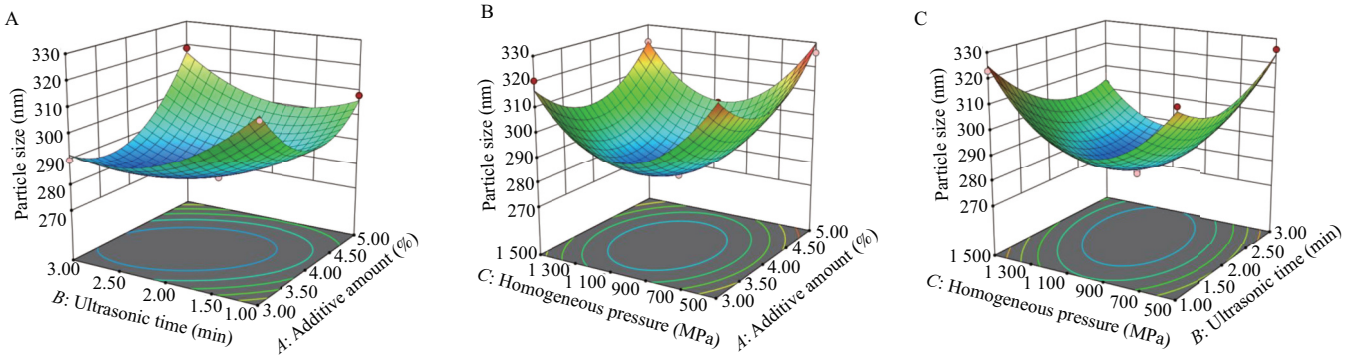

Fig. 1 Response surface diagram of the interaction between amount of emulsifier, ultrasonic time, and homogeneous pressure. (A) Amount of emulsifier and ultrasonic time. (B) Amount of emulsifier and homogeneous pressure. (C) Ultrasonic time and homogeneous pressure.

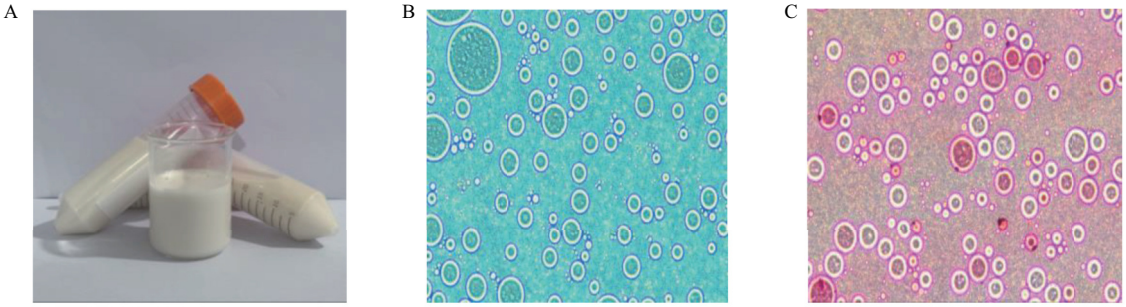

Fig. 2 Appearance, methylene blue and Sudan III staining of ASO-RRTJ/SE (200×). (A) Appearance. (B) Methylene blue staining. (C) Sudan III staining.

size of ASO-RRTJ/SE was (276.86 ± 4.61) nm and the PDI was 0.22 ± 0.02, less than 0.3, indicating that the ASO-RRTJ/SE had a narrow size distribution. The Zeta potential serves as an indicator of the degree of electrostatic repulsion or attraction exhibited between particles. It is an important index to characterize the stability of colloidal dispersion system. The Zeta potentials of ASO-RRTJ/SE was negative, and the absolute values were (30.57 ± 2.38) mV, which indicated that it had good physical stability.

Table 4 indicates that ASO-RRTJ/SE remains stable in a low-temperature environment. However, with increasing temperature, both its particle size and PDI gradually increase. Visually, when stored at 4 °C, ASO-RRTJ/SE maintains a uniform, light yellow emulsified liquid appearance until the 15th day. When stored at 20 °C, its appearance remains stable until the 10th day, but by the 15th day, a small amount of yellow precipitate appears. Under high-temperature conditions of 40 °C, yellow precipitate appears in ASO-RRTJ/SE on the 5th day, and oil-water separation occurs on the 10th day. This indicates that low temperatures are more favorable for the storage of ASO-RRTJ/SE.

3.4 Effect of ASO-RRTJ/SE on spatial memory in the MWM

The water maze test can not only evaluate animals' spatial memory, goal-directed behavior, and adaptability to the environment but also has important implications for studying animals' cognitive functions[26-27]. The MWM test was utilized to explore whether ASO-RRTJ/SE could alleviate the spatial learning and memory impairment caused by SCOP in mice. Table 5 shows that with the increase in training days from day 1 to day 5, the escape latency of mice in all groups gradually shortened during the navigation period. On the first day of training, compared to the Control group, mice treated with SCOP took longer to find the platform, indicating that SCOP treatment caused significant cognitive impairment in mice[28]. On day 2, compared to the Model group, the escape latency of mice in the DON, ASO, and ML groups was significantly shortened ($P < 0.05$). On day 3, compared to the Model group, the escape latency of the ASO, RRTJ, ML, and H-SE groups was shortened by 28.73%, 34.77%, 34.14%, and 37.34%, respectively, with no significant difference from the Control and DON groups. By day 5, the escape latency of mice in all groups had further shortened, with the ASO, ML, and H-SE groups performing even better, with escape latencies of 28.13, 27.30, and 26.13 s, respectively. Compared to the Model group, their escape latencies were shortened by 33.17%, 35.14%, and 37.92%, respectively, with no significant difference from the Control and DON groups.

Table 6 demonstrates that in the spatial exploration experiment, following 5 days of training, the time spent in the target quadrant significantly increased in the ASO (by 41.13%), ML (by 67.84%), M-SE (by 71.81%), and H-SE (by 70.57%) groups compared to the Model group ($P < 0.05$), there was no significant difference between the Control and DON groups. Nonetheless, there was not a significant difference in the quantity of platform crossings between the groups. Compared to the Model group, the proportion of the target quadrant distance traveled significantly increased in the ASO, ML, M-SE, and H-SE groups, by 69.96%, 67.90%, 71.81%, and 70.60%, respectively, showed no discernible variations from the Control and DON groups. The results of the MWM experiment indicate that scopolamine can cause damage to spatial learning and memory functions[29], while ASO-RRTJ/SE can improve learning and memory impairments caused by scopolamine.

3.5 Effects of ASO-RRTJ/SE on ACh and AChE activitie in the hippocampus

ACh is a vital essential neurotransmitter, while AChE is a key enzyme for the hydrolysis of ACh. The levels of ACh and the activity of AChE are crucial indicators for evaluating memory function[30-32].

The results of ACh levels and AChE activity in each group of mice are shown in Fig. 3. Compared to the Control group, the mice treated with SCOP showed a significant decrease in ACh levels and a remarkable increase in AChE activity in the hippocampus. Specifically, the Model group exhibited a 52.21% reduction in ACh levels and a 175%

Table 4
Changes of particle size and PDL of ASO-RRJ/SE under different storage temperatures and time.

Storage time (day)	4 °C		20 °C		40 °C	
	Particle size (nm)	Average PDI	Particle size (nm)	Average PDI	Particle size (nm)	Average PDI
0	277.56 ± 0.29	0.21 ± 0.07	276.77 ± 1.51	0.24 ± 0.06	278.31 ± 3.09	0.22 ± 0.05
5	278.50 ± 2.54	0.19 ± 0.04	281.44 ± 1.47	0.22 ± 0.01	293.55 ± 2.32	0.28 ± 0.04
10	281.30 ± 3.47	0.21 ± 0.04	283.30 ± 1.98	0.23 ± 0.03	301.56 ± 3.68	0.34 ± 0.06
15	280.70 ± 2.45	0.22 ± 0.02	283.40 ± 3.70	0.22 ± 0.03	335.70 ± 1.98	0.45 ± 0.14

Table 5
Effects of different groups on escape latency of MWM test in mice.

Group	Latency to find platform (s)				
	Day 1	Day 2	Day 3	Day 4	Day 5
Control	56.22 ± 10.33^{bA}	48.06 ± 16.89^{abA}	34.04 ± 22.80^{bB}	31.67 ± 21.80^{abB}	24.19 ± 21.34^{bB}
Model	60.00 ± 0.00^{aA}	58.86 ± 5.68^{aA}	53.99 ± 11.55^{aB}	45.57 ± 19.84^{aB}	42.09 ± 21.79^{aB}
DON	59.38 ± 2.50^{aA}	43.62 ± 17.39^{bB}	33.09 ± 20.94^{bBC}	25.45 ± 21.18^{Bbc}	$24.89 \pm 17.03^{b\,BC}$
ASO	60.00 ± 0.00^{aA}	47.26 ± 19.32^{bB}	38.48 ± 20.57^{bBC}	34.57 ± 23.16^{abBC}	28.13 ± 19.76^{bC}
RRTJ	59.34 ± 2.57^{aA}	51.02 ± 17.45^{abA}	35.22 ± 20.49^{bB}	34.95 ± 20.35^{abB}	31.11 ± 21.70^{abB}
ML	60.00 ± 0.00^{aA}	43.46 ± 18.72^{bB}	35.56 ± 20.70^{bBC}	35.49 ± 22.00^{abBC}	27.30 ± 19.08^{bC}
L-SE	60.00 ± 0.00^{aA}	52.87 ± 13.55^{abAB}	42.61 ± 20.27^{abBC}	38.10 ± 25.16^{abC}	31.34 ± 22.93^{abC}
M-SE	60.00 ± 0.00^{aA}	52.80 ± 15.74^{abAB}	43.46 ± 20.05^{abBC}	40.42 ± 20.21^{abCD}	31.35 ± 19.07^{abD}
H-SE	60.00 ± 0.00^{aA}	53.32 ± 10.90^{abA}	33.82 ± 20.23^{bB}	33.29 ± 22.37^{abB}	26.13 ± 19.80^{bB}

Note: Data are mean ± SD values. Different capital letters (A, B, C, D) on the same row represent significantly different from each other ($P < 0.05$); Different lowercase letters (a, b, c, d) on the same line represent significantly different from each other ($P < 0.05$).

Table 6
Effects of different groups on space exploration test in mice.

Group	Resident time in target quadrant (s)	Times of crossing the platform	Target distance percentage (%)
Control	17.08 ± 7.47^{ab}	3.27 ± 2.15	28.46 ± 12.44^{ab}
Model	11.35 ± 7.96^{b}	1.36 ± 1.36	18.91 ± 13.27^{b}
DON	18.99 ± 7.09^{a}	3.18 ± 2.04	31.65 ± 11.81^{a}
ASO	19.28 ± 6.32^{a}	2.91 ± 1.64	32.14 ± 10.55^{a}
RRTJ	17.26 ± 3.24^{ab}	2.45 ± 1.86	28.78 ± 5.39^{ab}
ML	19.05 ± 6.70^{a}	2.36 ± 1.86	31.75 ± 11.16^{a}
L-SE	14.87 ± 5.53^{ab}	2.36 ± 1.75	24.80 ± 9.20^{ab}
M-SE	19.50 ± 5.99^{a}	2.73 ± 2.00	32.49 ± 9.99^{a}
H-SE	19.36 ± 7.25^{a}	2.36 ± 1.80	32.26 ± 12.07^{a}

Note: Data are mean ± SD values. Different letters on the same line represent significantly different from each other ($P < 0.05$).

elevation in AChE activity, indicating cholinergic nervous system dysfunction in the Model group. Compared to the Model group, all treated groups showed a significant increase in hippocampal ACh levels. Among them, the L-SE, M-SE, and H-SE groups experienced increases of 34.39%, 53.26%, and 77.84% in ACh levels, respectively, demonstrating a dose-response relationship. The activity of the M-SE and H-SE groups was stronger than that of the ML (31.60%) group, and the H-SE group was comparable to the DON group.

Compared to the Model group, all treated groups showed a notable decrease in AChE activity. The reduction was relatively small in the ASO, RRTJ, and ML groups ($P < 0.05$). The L-SE, M-SE, and H-SE groups experienced reductions of 22.73%, 35.61%, and 46.97% in AChE activity, respectively, exhibiting a dose-response relationship. The activity of the L-SE group was similar to that of the ML (22.73%) group, while the activity of the M-SE and H-SE groups was stronger than that of the ML group. The H-SE group was comparable to the DON group (54.55%). The results suggest that supplementation with ASO-RRTJ/SE can prevent the imbalance of the cholinergic system induced by scopolamine in mice.

3.6 Effects of SE on the activity of SOD and the level of MDA in serum

SOD participates in redox reactions and is essential for removing free radicals from the system during antioxidant processes[33-34]. Because of its role as an antioxidant and in removing reactive oxygen species (ROS), SOD activity has gained increasing attention. These actions are thought to offer protection against a variety of diseases and aging processes linked to oxidative stress, including inflammation and neurodegeneration[35-36].

In organisms, free radicals induce peroxidation reactions in lipids, resulting in the production is MDA, which serves as a final oxidation product. MDA can cause cross-linking polymerization of large biological molecules such as proteins and nucleic acids, inhibit protein synthesis, and is cytotoxic[37]. Therefore, MDA content is an important parameter that reflects the potential antioxidant capacity, indicating the rate and intensity of lipid peroxidation and indirectly reflecting the degree of cell damage[38].

As shown in Fig. 4A, compared to the Control group, the SOD activity in the serum of mice in the Model group was significantly reduced by 30.68%, with a value of 67.24 U/mg pro. Compared to the Model group, all treated groups showed a significant increase in SOD activity, with the ML, M-SE, and H-SE groups showing the most prominent increases of 22.87%, 21.33%, and 29.48%, respectively, which were comparable to the DON group.

As illustrated in Fig. 4B, compared to the Control group, the MDA content in the serum of mice in the Model group increased significantly (81.53%). Compared to the Model group, the serum MDA levels in all treated groups were significantly reduced. The ML, M-SE, and H-SE groups had values of 6.66, 6.67, and 5.41 nmol/mL, respectively, representing reductions of 26.33%, 26.33%, and 40.15%. The activity of these groups was superior to that of the ASO (17.48%) and RRTJ (17.48%) groups. The L-SE, M-SE, and H-SE groups exhibited a dose-response relationship, with the H-SE group performing better than the ML group and showing no significant difference from the DON and Control groups. The findings show that consuming ASO-RRTJ/SE can significantly raise SOD activity and lower the amount of MDA in mice's serum.

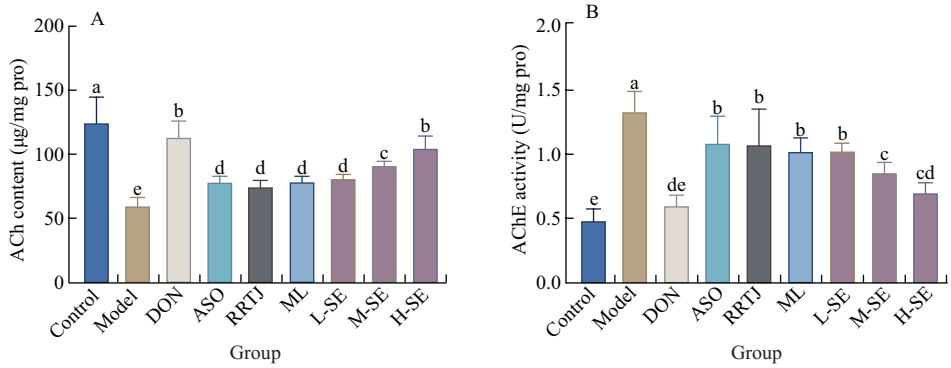

Fig. 3 Effects of different groups on ACh content and AChE activity in hippocampus of mice. (A) ACh content in hippocampus. (B) Hippocampal AChE activity. Different lowercase letters (a, b, c, d and e) means significantly different from each other ($P < 0.05$).

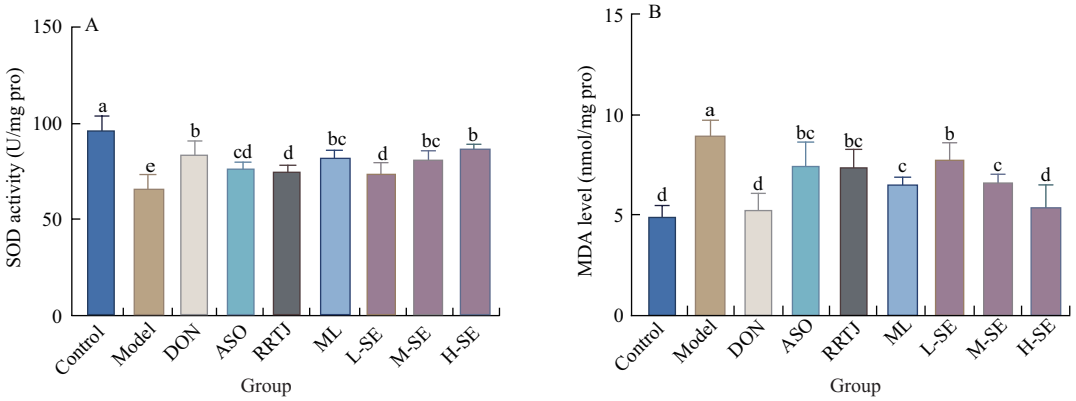

Fig. 4 Effects of different groups on SOD activity and MDA level in serum of mice. (A) SOD activity. (B) MDA level. Different lowercase letters (a, b, c, d and e) means significantly different from each other ($P < 0.05$).

3.7 Effects of ASO-RRTJ/SE on hippocampal morphology

The development and consolidation of learning and memory are significantly aided by the hippocampus in the brain[39-40]. Comprising the cornu ammonis 1 (CA1) cornu ammonis 3 (CA3), and dentate gyrus (DG) areas, the hippocampus plays a crucial role in the cholinergic system. The neuroprotective effects of ASO-RRTJ/SE on hippocampal neurons were observed through histopathological changes detected by H&E staining. Representative histopathological photomicrographs of H&E staining in the hippocampal CA1, CA3, and DG regions are shown in Fig. 5.

In the Control group, hippocampal neurons exhibited neatly arranged morphology, appearing normal and structurally intact. A relatively clear boundary was observed between the molecular layer and the outer granular layer, and the pyramidal cell layer was relatively normally arranged. However, in the Model group, some neuronal nuclei in the hippocampus showed pyknotic and deeply stained nuclei, cytoplasmic dissolution, and significantly widened intercellular distances in the areas indicated by arrows, where a large number of pyramidal cells appeared significantly smaller in size with pyknotic nuclei. The RRTJ group showed a small amount of pyknotic and deeply stained nuclei in the hippocampal region, while the ASO group only exhibited this condition in the CA1 and DG regions. In contrast, the SE group showed neatly arranged hippocampal neurons, reduced nuclear pyknosis, deeply stained nuclei, and cytoplasmic dissolution. The pyramidal cell layer was neatly arranged, and the intercellular distances returned to normal. The effect was even more prominent in the H-SE group. These results suggest that supplementation with ASO-RRTJ/SE can effectively alleviate scopolamine-induced damage to hippocampal nerve cells, maintain cell viability and integrity, and thereby improve memory ability in mice.

3.8. Effects of ASO-RRTJ/SE on protein expression in brain tissue of mice

To further validate the neuroprotective effects of ASO-RRTJ/SE on scopolamine- induced memory impairment, immunofluorescence staining was used to investigate the status of p-tau, ChAT, and BDNF in the hippocampus of mice.

Coronal sections of the hippocampus were stained with FITC-labeled p-tau antibodies. Given that tau predominantly exists in neurons, immunofluorescence analysis employed to ascertain the distribution of p-tau in hippocampal neurons, with DAPI used for counterstaining the hippocampus. As shown in Figs. 6 and 7A, there are only a very small number of aggregates in the control group of mice, while an increase in p-tau protein aggregation occurs in scopolamine-induced mice, with the model group being the most severe, increased by 183.60% compared to the Control group. This suggests that in addition to inducing memory impairment by causing an imbalance in the cholinergic system of mice, the aggregation of p-tau protein may also be one of the reasons for memory impairment[41-42]. Compared to the Model group, mice in the ML,

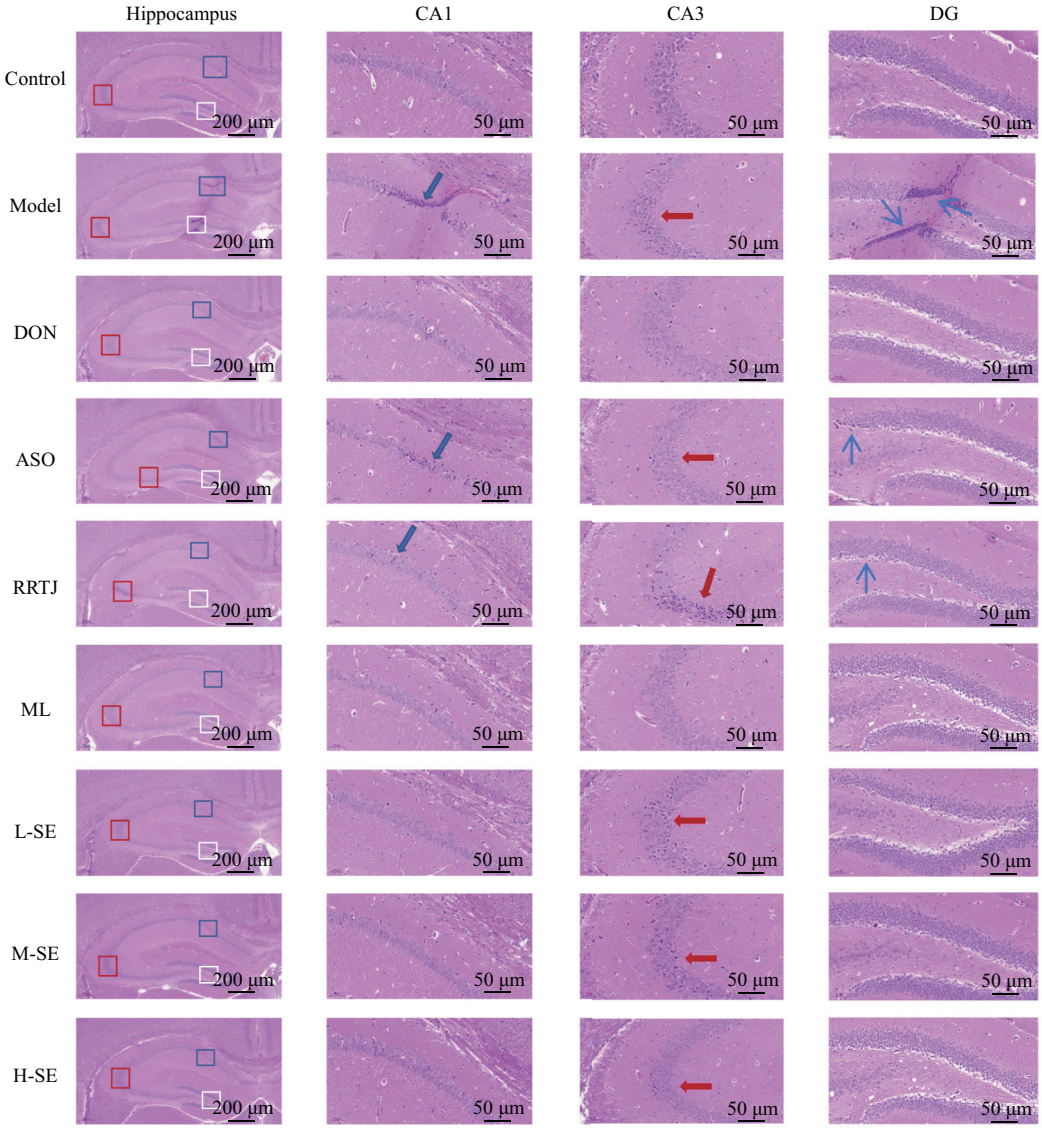

Fig. 5 Pathological sections of the hippocampal CA1, CA3 and DG region stained with H&E of different groups, scale bar: 200 or 50 μm. In the hippocampal diagram, different colored boxes represent different regions of the hippocampus, with blue representing the CA1 region, red representing the CA3 region, and white representing the DG region.

M-SE, and H-SE groups all exhibited significant reductions in p-tau protein aggregation ($P < 0.05$). Among them, M-SE and H-SE showed a certain dose-effect relationship, with H-SE demonstrating the most pronounced effect, showing no significant difference from the DON group and the Control group.

A key player in memory, learning, and the growth and differentiation of dendrites and neurons, the cholinergic system is regarded as one of the most significant systems in the brain's neurotransmitter system[43-45]. A decrease in the neurotransmitter ACh leads to a lack of learning and memory, and ChAT is the biosynthetic enzyme for ACh[46]. Therefore, the expression level of ChAT enzyme in the mouse hippocampus can be analyzed to investigate whether ASO-RRTJ/SE can improve memory impairment by enhancing cholinergic signaling in the hippocampus.

As observed in Figs. 6 and 7B, the expression of ChAT in the Model group significantly decreased compared with the Control group, reaching only 58.71% of the Control group. Conversely, compared with the Model group, the expression of ChAT was significantly increased in the ML, M-SE, and H-SE groups ($P < 0.05$), with the M-SE and H-SE groups displaying a discernible dose-effect relationship. The H-SE group was superior to the ML group and showed no significant difference from the DON group. The expression of ChAT in each group further illustrates that scopolamine induces memory impairment by causing an imbalance in the cholinergic system of mice, which is consistent with data on ACh content and AChE activity in the mouse hippocampus. The results indicate that ASO-RRTJ/SE can improve memory impairment by enhancing cholinergic signaling in the hippocampus.

BDNF is one of the neurotrophins that have a significant impact on neural survival and differentiation[47-48]. It can affect the growth and development of brain nerves through its neurotrophic effects, promote neurogenesis in the hippocampus, and influence learning and memory functions[49-52]. As shown in Figs. 6 and 7C, there was barely any BDNF in the Model group and a little quantity in the

Control group. The groups that swallowed ASO, ML, ASO, M-SE, and H-SE had significantly greater BDNF-positive cell rates than the Model group, with the H-SE group having significantly higher rates than the Control group. This may be related to the presence of nervonic acid in ASO. As one of the functional fatty acids, nervonic acid has the ability to stimulate neurons to produce a substance known as BDNF. This substance plays a crucial role in promoting the regeneration and repair of damaged nerve fibers[6,53]. In addition, vitamin E, which is rich in ASO, can reduce oxidative stress and increase BDNF expression in hippocampus of rats[54-55]. Therefore, we speculate that the intake of ASO-RRTJ/SE is beneficial for the production of BDNF in the hippocampus.

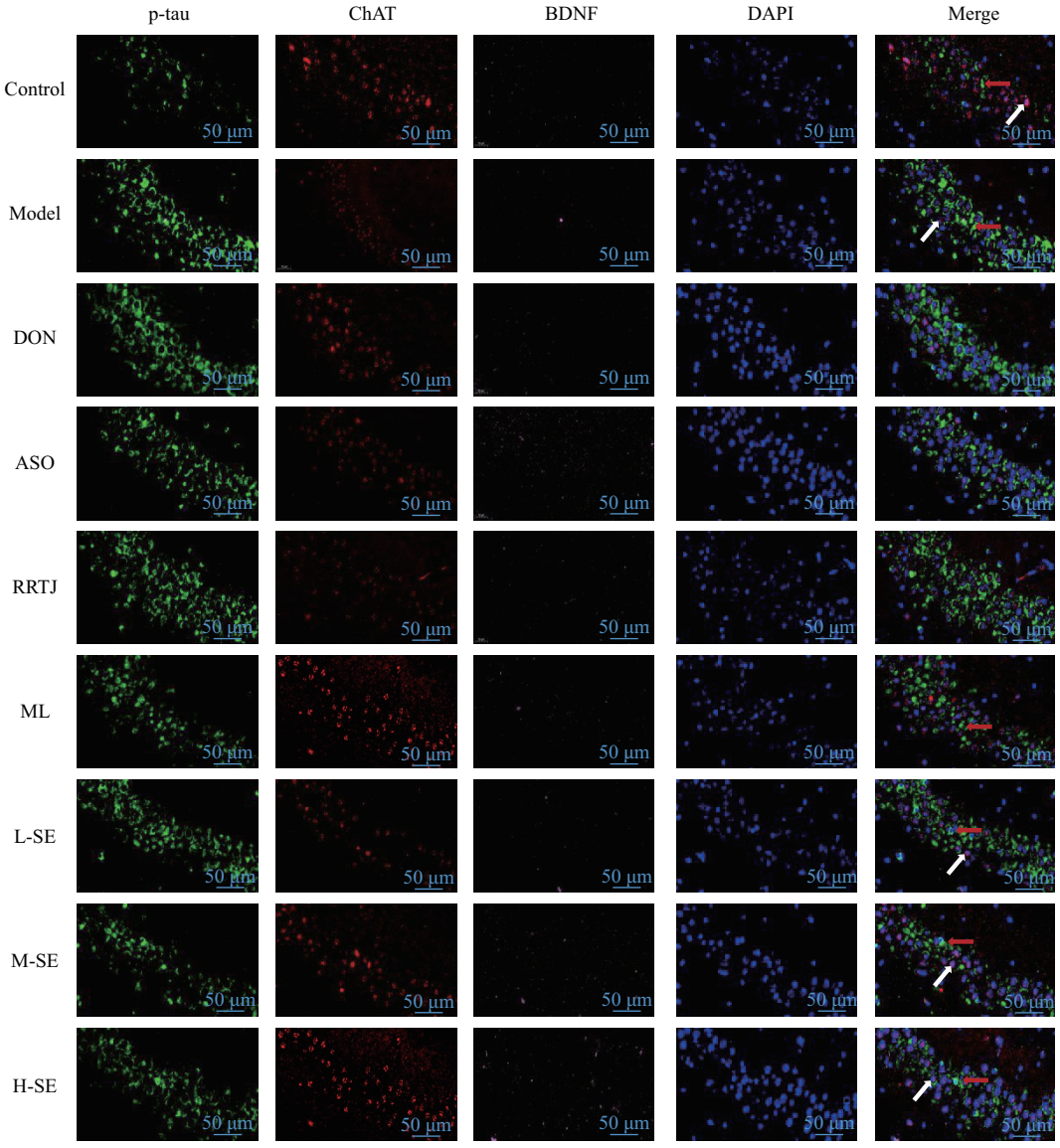

Fig. 6 Different colored arrows represent different antibodies, with red indicating p-tau antibody expression and white representing ChAT expression. Scale bar: 50 μm.

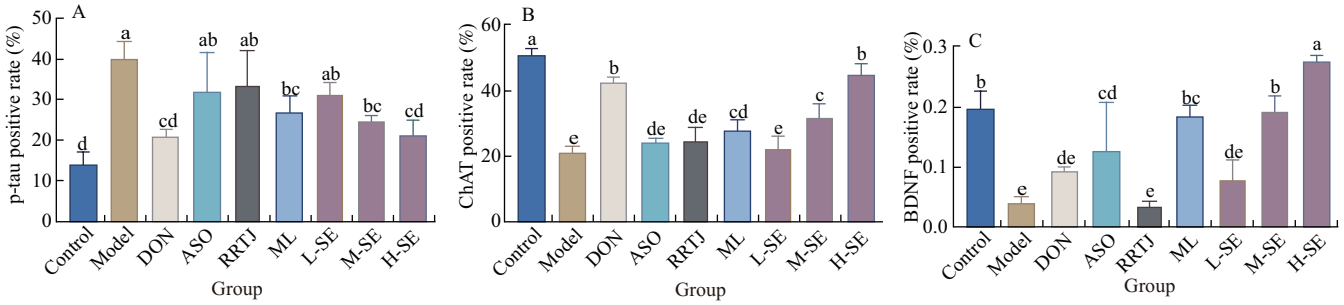

Fig. 7 Positive rate of p-tau, ChAT and BDNF. (A) p-tau. (B) ChAT. (C) BDNF. Different lowercase letters (a, b, c, d and e) means significantly different from each other ($P < 0.05$).

4. Conclusion

In this study, we successfully prepared a submicron emulsion of ASO and RRTJ through formula screening, cell disruption, and micro-jet homogenization. Optimal preparation conditions were attained *via* response surface optimization. Analysis of particle size, PDI, Zeta potential, *K*e value, and centrifugal retention rate affirmed the stability of ASO-RRTJ/SE as an oral formulation. We employed a mouse model of memory dysfunction to perform a thorough examination into the impact of ASO-RRTJ/SE on scopolamine-induced memory impairment. Evaluation of behavioral indicators, ACh content, AChE activity, SOD activity, and MDA levels revealed significantly enhanced memory abilities in mice treated with ASO-RRTJ/SE compared to memory-impaired mice. Yet, in the examination of behavior, it is not conclusive that the submicron emulsion formulation of ASO and RRTJ improves memory more effectively than the ASO and RRTJ mixture. Furthermore, the SE group exhibited neatly arranged hippocampal neurons, reversing nuclear pyknosis, deep staining, and cytoplasmic dissolution. The pyramidal cell layer appeared more organized, and intercellular distances returned to normal, effectively reducing hippocampal neuronal damage caused by scopolamine and maintaining cellular viability and integrity. ASO-RRTJ/SE significantly reduced the aggregation of phosphorylated tau protein in the mouse hippocampus, increased ChAT expression, and promoted BDNF production. In conclusion, ASO-RRTJ/SE demonstrates enhanced efficacy in improving memory. This study presents a promising avenue for the development and utilization of *A. truncatum* and RRT resources, as well as for the research and development of functional and diversified products derived from ASO.

Declaration of competing interest

The authors declare that they have no known competing financial interests or personal relationships that could have appeared to influence the work reported in this paper.

Acknowledgements

This work was supported by grants from Science and Technology Support Program of Guizhou Province (Qian Ke He Zhi Cheng-[2021]127 and [2024]097; Qian Ke He Foundation-ZK-[2023]General 242).

References

[1] Y. Fan, F. Lin, R. Zhang, et al., *Acer truncatum* Bunge: a comprehensive review on ethnobotany, phytochemistry and pharmacology, J. Ethnopharmacol. 282 (2022) 114572. https://doi.org/10.1016/j.jep.2021.114572.

[2] X. He, D.Z. Li, B. Tian, Diversity in seed oil content and fatty acid composition in *Acer* species with potential as sources of nervonic acid, Plant Divers. 43 (2021) 86-92. https://doi.org/10.1016/j.pld.2020.10.003.

[3] Y. Fan, H.M. Meng, G.R. Hu, et al., Biosynthesis of nervonic acid and perspectives for its production by microalgae and other microorganisms, Appl. Microbiol. Biotechnol. 102 (2018) 3027-3035. https://doi.org/10.1007/s00253-018-8859-y.

[4] Q. Ma, T. Sun, S. Li, et al., The *Acer truncatum* genome provides insights into nervonic acid biosynthesis, Plant J. 104 (2020) 662-678. https://doi.org/10.1111/tpj.14954.

[5] X.Y. Chen, Y.G. Song, W.T. Song, et al., Multi-omics reveal neuroprotection of *Acer truncatum* Bunge Seed extract on hypoxic-ischemia encephalopathy rats under high-altitude, Commun. Biol. 6 (2023) 1001. https://doi.org/10.1038/s42003-023-05341-9.

[6] X. Li, T. Li, X.Y. Hong, et al., *Acer truncatum* seed oil alleviates learning and memory impairments of aging mice, Front. Cell Dev. Biol. 9 (2021) 680386. https://doi.org/10.3389/fcell.2021.680386.

[7] W. Song, K. Zhang, T. Xue, et al., Cognitive improvement effect of nervonic acid and essential fatty acids on rats ingesting *Acer truncatum* Bunge seed oil revealed by lipidomics approach, Food Funct. 13 (2022) 2475-2490. https://doi.org/10.1039/d1fo03671h.

[8] Y. Xue, X. Zhu, W. Yan, et al., Dietary supplementation with *Acer truncatum* oil promotes remyelination in a mouse model of multiple sclerosis, Front. Neurosci. 16 (2022) 860280. https://doi.org/10.3389/fnins.2022.860280.

[9] J.E. Slemmer, J.J. Shacka, M.I. Sweeney, et al., Antioxidants and free radical scavengers for the treatment of stroke, traumatic brain injury and aging, Curr. Med. Chem. 15 (2008) 401-414. https://doi.org/10.2174/092986708783497337.

[10] L. Zhu, C. Sun, J. Ren, et al., Stress-induced precocious aging in PD-patient iPSC-derived NSCs may underlie the pathophysiology of Parkinson's disease, Cell Death Dis. 10 (2019) 105. https://doi.org/10.1038/s41419-019-1313-y.

[11] L. Wang, T. Wei, L. Zheng, et al., Recent advances on main active ingredients, pharmacological activities of *Rosa roxbughii* and its development and utilization, Foods 12 (2023) 1051. https://doi.org/10.3390/foods12051051.

[12] Y. Li, F. Chen, X. Liu, Effects of *Rosa roxburghii* Tratt must on the growth, nutrient composition, and antioxidant activity of *Pleurotus ostreatus* mycelia, Molecules 27 (2022) 3585. https://doi.org/10.3390/molecules27113585.

[13] J.C. Ji, S. Zhang, L. Tang, et al., Integrative analysis of fecal metabolome and gut microbiota in high-fat diet-induced hyperlipidemic rats treated with *Rosa roxburghii* Tratt juice, J. Func. Foods 90 (2022) 104978. https://doi.org/10.1016/j.jff.2022.104978.

[14] S. Yang, X.Y. Huang, N. Zhou, et al., RNA-Seq analysis of protection against chronic alcohol liver injury by *Rosa roxburghii* fruit juice (Cili) in mice, Nutrients 14 (2022) 1974. https://doi.org/10.3390/nu14091974.

[15] Q. Ma, Y. Wang, S. Li, et al., Assembly and comparative analysis of the first complete mitochondrial genome of *Acer truncatum* Bunge: a woody oil-tree species producing nervonic acid, BMC Plant Biol. 22 (2022) 29. https://doi.org/10.1186/s12870-021-03416-5.

[16] H. Karami, M. Rasekh, E. Mirzaee-Ghaleh, Qualitative analysis of edible oil oxidation using an olfactory machine, J. Food Meas. Charact. 14 (2020) 2600-2610. https://doi.org/10.1007/s11694-020-00506-0.

[17] Y. Qi, Y. Huang, Y. Dong, et al., Effective improvement of the oxidative stability of *Acer truncatum* Bunge seed oil, a new woody oil food resource, by rosemary extract, Antioxidants 12 (2023) 889. https://www.mdpi.com/2076-3921/12/4/889.

[18] Y. Xie, J. Chen, S. Zhang, et al., The research about microscopic structure of emulsion membrane in O/W emulsion by NMR and its influence to emulsion stability, International Journal of Pharmaceutics 500 (2016) 110-119. https://doi.org/10.1016/j.ijpharm.2016.01.032.

[19] Y. Song, H. Gao, S. Zhang, et al., Prescription optimization and oral bioavailability study of salvianolic acid extracts W/O/W multiple emulsion, Biol. Pharm. Bull. 40 (2017) 2081-2087. https://doi.org/10.1248/bpb.b17-00162.

[20] X. Lin, C.Y. Zhao, R. Dong, et al., Hematological metabonomics study of naringin improving learning cognitive ability of scopolamine model mice, Chin. J. Pharm. Anal. 42 (2022) 263-270. https://doi.org/10.16155/j.0254-1793.2022.02.10.

[21] J. Zheng, Y. Gao, J. Ding, et al., Antarctic krill peptides improve scopolamine-induced memory impairment in mice, Food Biosci. 49 (2022) 101987. https://doi.org/https://doi.org/10.1016/j.fbio.2022.101987.

[22] P. Ataeian, R. Nasseri, A. Tong, et al., Effect of oil phase transition on the stability of Pickering emulsions stabilized by cellulose nanocrystals, Langmuir. 38 (2022) 2737-2745. https://doi.org/10.1021/acs.langmuir.2c00107.

[23] I. Abcha, S. Souilem, M.A. Neves, et al., Ethyl oleate food-grade O/W emulsions loaded with apigenin: insights to their formulation characteristics and physico-chemical stability, Food Res. Int. 116 (2019) 953-962. https://doi.org/10.1016/j.foodres.2018.09.032.

[24] V. Mundada, M. Patel, K. Sawant, Submicron emulsions and their applications in oral delivery, Crit. Rev. Ther. Drug Carrier. Syst. 33 (2016) 265-308. https://doi.org/10.1615/CritRevTherDrugCarrierSyst.2016017218.

[25] E.C. Giakoumatos, A. Aloi, I.K. Voets, Illuminating the impact of submicron particle size and surface chemistry on interfacial position and Pickering emulsion type, Nano Lett. 20 (2020) 4837-4841. https://doi.org/10.1021/acs.nanolett.0c00709.

[26] K. Bromley-Brits, Y. Deng, W. Song, Morris water maze test for learning and memory deficits in Alzheimer's disease model mice, J. Vis. Exp. 20 (2011) 2920. https://doi.org/10.3791/2920.

[27] M.Z. Othman, Z. Hassan, A.T. Che Has, Morris water maze: a versatile and pertinent tool for assessing spatial learning and memory, Exp. Anim. 71 (2022) 264-280. https://doi.org/10.1538/expanim.21-0120.

[28] K. Khurana, M. Kumar, N. Bansal, Lacidipine prevents scopolamine-induced memory impairment by reducing brain oxido-nitrosative stress in mice, Neurotox. Res. 39 (2021) 1087-1102. https://doi.org/10.1007/s12640-021-00346-w.

[29] H.S. Park, E.S. Hwang, G.Y. Choi, et al., Sulforaphane enhances long-term potentiation and ameliorate scopolamine-induced memory impairment, Physiol. Behav. 238 (2021) 113467. https://doi.org/10.1016/j.physbeh.2021.113467.

[30] T.H. Ferreira-Vieira, I.M. Guimaraes, F.R. Silva, et al., Alzheimer's disease: targeting the cholinergic system, Curr. Neuropharmacol. 14 (2016) 101-115. https://doi.org/10.2174/1570159x13666150716165726.

[31] M.C. Krawczyk, J. Millan, M.G. Blake, et al., Critical role of hippocampal muscarinic acetylcholine receptors on memory reconsolidation in mice, Neurobiol. Learn Mem. 177 (2021) 107360. https://doi.org/10.1016/j.nlm.2020.107360.

[32] C. Stein, K. Koch, J. Hopfeld, et al., Impaired hippocampal and thalamic acetylcholine release in P301L tau-transgenic mice, Brain Res. Bull. 152 (2019) 134-142. https://doi.org/10.1016/j.brainresbull.2019.07.014.

[33] T.T. Huang, D. Leu, Y. Zou, Oxidative stress and redox regulation on hippocampal- dependent cognitive functions, Arch. Biochem. Biophys. 57 (2015) 2-7. https://doi.org/10.1016/j.abb.2015.03.014.

[34] A. Sha, Y. Liu, X. Qiu, et al., Polysaccharide from *Paris polyphylla* improves learning and memory ability in *D*-galactose-induced aging model mice based on antioxidation, p19/p53/p21, and Wnt/*β*-catenin signaling pathways, Int. J. Biol. Macromol. 251 (2023) 126311. https://doi.org/10.1016/j.ijbiomac.2023.126311.

[35] N.A. Estrada-Cruz, L. Manuel-Apolinar, J.J. Segura-Uribe, et al., Short-term administration of tibolone reduces inflammation and oxidative stress in the hippocampus of ovariectomized rats fed high-fat and high-fructose, Nutr. Neurosci. 26 (2023) 275-289. https://doi.org/10.1080/1028415x.2022.2046964.

[36] H.M. Hussien, D.A. Ghareeb, H.E.A. Ahmed, et al., Pharmacological implications of ipriflavone against environmental metal-induced neurodegeneration and dementia in rats, Environ. Sci. Pollut. Res. Int. 28 (2021) 65349-65362. https://doi.org/10.1007/s11356-021-15193-7.

[37] X. Wang, X. Chen, G. Liu, et al., The crucial roles of pitx3 in midbrain dopaminergic neuron development and Parkinson's disease-associated neurodegeneration, Int. J. Mol. Sci. 24 (2023) 8614. https://doi.org/10.3390/ijms24108614.

[38] F. Norouzi, M. Hosseini, A. Abareshi, et al., Memory enhancing effect of Nigella Sativa hydro-alcoholic extract on lipopolysaccharide-induced memory impairment in rats, Drug Chem. Toxicol. 42 (2019) 270-279. https://doi.org/10.1080/01480545.2018.1447578.

[39] T. Bartsch, P. Wulff, The hippocampus in aging and disease: from plasticity to vulnerability, Neuroscience 309 (2015) 1-16. https://doi.org/10.1016/j.neuroscience.2015.07.084.

[40] L. Colucci-D'Amato, L. Speranza, F. Volpicelli, Neurotrophic factor BDNF, physiological functions and therapeutic potential in depression, neurodegeneration and brain cancer, Int. J. Mol. Sci. 21 (2020) 7777. https://doi.org/10.3390/ijms21207777.

[41] P. Katiyar, A. Singh Rathore, S. Banerjee, et al., Wheatgrass extract imparts neuroprotective actions against scopolamine-induced amnesia in mice, Food Funct. 13 (2022) 8474-8488. https://doi.org/10.1039/d2fo00423b.

[42] R. Ossenkoppele, R. van der Kant, O. Hansson, Tau biomarkers in Alzheimer's disease: towards implementation in clinical practice and trials, Lancet Neurol. 21 (2022) 726-734. https://doi.org/10.1016/s1474-4422(22)00168-5.

[43] B. Balkan, S. Pogun, Nicotinic cholinergic system in the hypothalamus modulates the activity of the hypothalamic neuropeptides during the stress response, Curr. Neuropharmacol. 16 (2018) 371-387. https://doi.org/10.2174/1570159x15666170720092442.

[44] J. Peter, J. Lahr, L. Minkova, et al., Contribution of the cholinergic system to verbal memory performance in mild cognitive impairment, J. Alzheimers Dis. 53 (2016) 991-1001. https://doi.org/10.3233/jad-160273.

[45] N. Solari, B. Hangya, Cholinergic modulation of spatial learning, memory and navigation, Eur. J. Neurosci. 48 (2018) 2199-2230. https://doi.org/10.1111/ejn.14089.

[46] J.H. Choi, E.B. Lee, H.H. Jang, et al., *Allium hookeri* extracts improve scopolamine-induced cognitive impairment *via* activation of the cholinergic system and anti-neuroinflammation in mice, Nutrients 13 (2021) 2890. https://doi.org/10.3390/nu13082890.

[47] M. Aragona, C. Porcino, M.C. Guerrera, et al., The BDNF/TrkB neurotrophin system in the sensory organs of zebrafish, Int. J. Mol. Sci. 23 (2022) 2621. https://doi.org/10.3390/ijms23052621.

[48] G. Leal, C.R. Bramham, C.B. Duarte, BDNF and hippocampal synaptic plasticity, Vitam. Horm. 104 (2017) 153-195. https://doi.org/10.1016/bs.vh.2016.10.004.

[49] M. Banerjee, R.R. Shenoy , Emphasizing roles of BDNF promoters and inducers in Alzheimer's disease for improving impaired cognition and memory, J. Basic Clin. Physiol. Pharmacol. 34 (2023) 125-136. https://doi.org/10.1515/jbcpp-2021-0182.

[50] M. Hosseini, F. Mansouritorghabeh, F. Beheshti, et al., Capparis spinosa promoted BDNF and antioxidant enzyme levels to protect against learning and memory deficits induced by scopolamine, Cent. Nerv. Syst. Agents. Med. Chem. 23 (2023) 109-118. https://doi.org/10.2174/1871524923666230719121439.

[51] M. Sasi, B. Vignoli, M. Canossa, et al., Neurobiology of local and intercellular BDNF signaling, Pflug. Arch. Eur. J. Phy. 469 (2017) 593-610. https://doi.org/10.1007/s00424-017-1964-4.

[52] L. Xu, L.N. Zhu, L.N. Zhu, et al., Moderate exercise combined with enriched environment enhances learning and memory through BDNF/TrkB signaling pathway in rats, Int. J. Environ. Res. Public Health 18 (2021) 82-82. https://doi.org/10.3390/ijerph18168283.

[53] Y.C. Chung, Y. Cui, T. Sumiyoshi, et al., Associations of fatty acids with cognition, psychopathology, and brain-derived neurotrophic factor levels in patients with first-episode schizophrenia and related disorders treated with paliperidone extended release, J. Psychopharmacol. 31 (2017) 1556-1563. https://doi.org/10.1177/0269881117731169.

[54] J.J. Wei, S.T. Zhao, Progress on active ingredients and application of *Acer truncatum* Bunge, Progressin Veterinary Medicine 42 (2021)105-109.

[55] A.A. Altarifi, K. Sawali, K.H. Alzoubi, et al., Effect of vitamin E on doxorubicin and paclitaxel-induced memory impairments in male rats, Cancer Chemoth. Pharm. 93 (2024) 215-224.